



HAL
open science

Accidental eccentricity in symmetric buildings due to wave passage effects arising from near-fault pulse-like ground motions

Yenan Cao, George Mavroeidis, Kristel Carolina Meza Fajardo, Apostolos Papageorgiou

► To cite this version:

Yenan Cao, George Mavroeidis, Kristel Carolina Meza Fajardo, Apostolos Papageorgiou. Accidental eccentricity in symmetric buildings due to wave passage effects arising from near-fault pulse-like ground motions. *Earthquake Engineering and Structural Dynamics*, 2017, 46 (13), pp.2185 - 2207. 10.1002/eqe.2901 . hal-01817956

HAL Id: hal-01817956

<https://brgm.hal.science/hal-01817956>

Submitted on 6 Dec 2022

HAL is a multi-disciplinary open access archive for the deposit and dissemination of scientific research documents, whether they are published or not. The documents may come from teaching and research institutions in France or abroad, or from public or private research centers.

L'archive ouverte pluridisciplinaire **HAL**, est destinée au dépôt et à la diffusion de documents scientifiques de niveau recherche, publiés ou non, émanant des établissements d'enseignement et de recherche français ou étrangers, des laboratoires publics ou privés.

Accidental eccentricity in symmetric buildings due to wave passage effects arising from near-fault pulse-like ground motions

Yenan Cao¹, George P. Mavroeidis^{1,*} , Kristel C. Meza-Fajardo² and Apostolos S. Papageorgiou³

¹*Department of Civil and Environmental Engineering and Earth Sciences, University of Notre Dame, Notre Dame, IN 46556, U.S.A.*

²*Risks and Prevention Division, Seismic and Volcanic Risks Unit, BRGM, 45060 Orleans Cedex 02, France*

³*Department of Civil Engineering, University of Patras, Patras 26500, Greece*

SUMMARY

This article investigates the characteristics of the accidental eccentricity in symmetric buildings due to torsional response arising from wave passage effects in the near-fault region. The soil–foundation–structure system is modeled as a symmetric cylinder placed on a rigid circular foundation supported on an elastic halfspace and subjected to obliquely incident plane SH waves simulating the action of near-fault pulse-like ground motions. The translational response is computed assuming that the superstructure behaves as a shear beam under the action of translational and rocking base excitations, whereas the torsional response is calculated using the mathematical formulation proposed in a previous study. A broad range of properties of the soil–foundation–structure system and ground motion input are considered in the analysis, thus facilitating a detailed parametric investigation of the structural response. It is demonstrated that the normalized accidental eccentricity is most sensitive to the pulse period (T_P) of the near-fault ground motions and to the uncoupled torsional-to-translational fundamental frequency ratio (Ω) of the structure. Furthermore, the normalized accidental eccentricities due to simplified pulse-like and broadband ground motions in the near-fault region are computed and compared against each other. The results show that the normalized accidental eccentricity due to the broadband ground motion is well approximated by the simplified pulse for longer period buildings, while it is underestimated for shorter period buildings. For symmetric buildings with values of Ω commonly used in design practice, the normalized accidental eccentricity due to wave passage effects is less than the typical code-prescribed value of 5%, except for buildings with very large foundation radius. Copyright © 2017 John Wiley & Sons, Ltd.

Received 25 October 2016; Revised 3 March 2017; Accepted 6 March 2017

KEY WORDS: near-fault ground motion; translational and torsional response; soil–structure interaction; wave passage effects; accidental eccentricity

1. INTRODUCTION

Earthquake-induced torsion in buildings can be classified into ‘natural’ and ‘accidental’. The natural (or inherent) torsion is induced by the geometrical separation of the centers of mass and stiffness, resulting in coupled lateral–torsional response. On the other hand, the accidental torsion is associated with torsional vibrations generated by spatially varying seismic excitations, uncertainties in the distributions of stiffness and mass, and other factors that are not explicitly considered in the analysis and design of buildings.

*Correspondence to: George P. Mavroeidis, Department of Civil and Environmental Engineering and Earth Sciences, 156 Fitzpatrick Hall, University of Notre Dame, Notre Dame, IN 46556, U.S.A.

†E-mail: g.mavroeidis@nd.edu

Most building codes require the effects of accidental torsion to be considered by applying the equivalent static lateral force at a distance e_a from the center of stiffness, resulting in accidental torsional moments that are typically resisted by increasing the design shear forces in the lateral resisting system. The quantity e_a , also known as design accidental eccentricity, is usually defined in building codes as a fraction (e.g. 5% or 10%) of the building dimension. Several studies have investigated the effects of spatially varying seismic excitations (resulting from ground motion incoherence and wave passage) on the torsional response of buildings and evaluated the adequacy of the accidental eccentricity prescribed by building codes, but only a few are summarized in this section. The interested reader is referred to Anagnostopoulos et al. [1] for a comprehensive literature review of accidental torsion in buildings.

Newmark [2] made the first rational attempt to investigate the torsional response of symmetric buildings due to base rotations arising from earthquake waves propagating with a constant velocity. It was concluded that the ratio of the design accidental eccentricity to the long plan dimension of the building varies directly with the fundamental frequency of vibration and with the transit time of the earthquake wave motion across the long plan dimension. Luco [3] presented the mathematical formulation of the torsional response of a symmetric, elastic structure placed on a surface-supported foundation under the action of obliquely incident plane SH waves, while accounting for soil–structure interaction (SSI) effects. It was demonstrated that large displacements associated with torsional response may be generated even for symmetric structures. Luco and Sotiropoulos [4] investigated the effects of wave passage on the torsional response of a square foundation and showed that an accidental eccentricity of 5% is sufficient to account for the effects of wave passage on structures with a fundamental frequency less than 5 Hz and foundation length in the direction of propagation less than 40 m. For structures with fundamental frequency and foundation length not satisfying these conditions or for structures located at short distances from the seismic source, it was determined that the accidental eccentricity can be greater than 5%.

Morgan et al. [5] investigated the translational and torsional response of buildings arising from traveling waves using strong motion data. They showed that the effects of induced rotations on structures are not important for fundamental frequencies less than 1 Hz and the 5% accidental eccentricity specified in building codes is adequate. Wu and Leyendecker [6] examined the torsional response of a single-storey system subjected to an incident SH wave and concluded that the effects of accidental eccentricity on the dynamic response of symmetric buildings cannot be ignored. De la Llera and Chopra [7] extracted base torsional excitations, associated with spatially varying ground motions, from translational recordings at the foundation level of actual buildings. They demonstrated that the increase in building displacements resulting from accidental torsion due to the extracted torsional excitations may be large for short-period (i.e. less than 0.5 s) and torsionally flexible systems. In addition, the computed accidental eccentricities were found to be significantly smaller than the typical code values, except for buildings with very long plan dimensions (i.e. greater than 50 m).

Heredia-Zavoni and Barranco [8] examined the torsional response of symmetric structural systems subjected to spatially varying ground motions due to ground motion incoherence, wave passage, and local soil conditions. It was demonstrated that the accidental eccentricity may exceed the standard code-prescribed values of 5 and 10% depending on the period and aspect ratio of the system, the local soil conditions, and the times for the seismic waves to travel across the base of the system. Heredia-Zavoni and Leyva [9] investigated the effects of ground motion incoherence and wave passage on the torsional response of three-dimensional, multi-storey, multi-span, symmetric, linear elastic buildings. They showed that the use of a base shear along with the design accidental eccentricity specified in the building code for Mexico City may result in considerably high estimates of shear force in corner columns of structures on firm soil; however, for soft soil conditions, the shear force in corner columns may be underestimated, especially for short-period buildings with long plan dimensions. Aviles and Suarez [10] evaluated the natural and accidental torsion in a single monosymmetric structure with consideration of SSI. The structure was placed on a rigid foundation embedded into an elastic halfspace, whereas the earthquake excitation was assumed to be composed of non-vertically incident SH waves. By considering different combinations of the system parameters and an ensemble of ground motion records, it was demonstrated that the computed accidental

eccentricity does not exceed the smallest codified value of 5% except for surface-supported structures with long plan dimensions.

In a recent study, Cao et al. [11] investigated the effects of wave passage on the torsional response of symmetric buildings in the near-fault region. The soil–foundation–structure system was modeled as a symmetric cylinder placed on a rigid circular foundation supported on an elastic halfspace and subjected to obliquely incident plane SH waves simulating the action of near-fault pulse-like ground motions. A detailed parametric analysis of the maximum relative twist between the top and the base of the superstructure was performed to identify the parameters of the seismic excitation input and soil–foundation–structure system that control the torsional response. It was shown that large torsional response is observed when a key parameter of the near-fault ground motions referred to as ‘pulse period’ is close to the fundamental torsional period of the structure.

Building upon the results of Cao et al. [11], this article aims to further evaluate the increase in building displacements due to the torsional response arising from wave passage effects in the near-fault region. This is achieved by comparing the accidental eccentricity, estimated from the translational and torsional components of the building response, with code-prescribed values. The translational response is computed using a closed-form expression derived in the present study assuming that the superstructure behaves as a shear beam under the action of translational and rocking base excitations, whereas the torsional response is calculated using the mathematical formulation proposed by Luco [3]. A broad range of properties of the soil–foundation–structure system and ground motion input are considered in the analysis, thus facilitating a detailed parametric investigation. Finally, the effectiveness of idealized pulse models to accurately estimate the accidental eccentricity for symmetric buildings arising from wave passage effects in the near-fault region is assessed by estimating and comparing the accidental eccentricities due to simplified pulse-like and broadband ground motions.

2. NEAR-FAULT PULSE-LIKE GROUND MOTIONS

Forward rupture directivity and/or permanent translation (fling) are the two primary physical processes that give rise to pulse-like ground motions in the near-fault region. In this study, the mathematical model proposed by Mavroeidis and Papageorgiou [12] is adopted to describe the coherent component of the near-fault ground motions. The formulation of the mathematical model for the ground velocity pulses is the product of a harmonic oscillation and a bell-shaped function:

$$v(t) = \begin{cases} \frac{A}{2} \left[1 + \cos \left(\frac{2\pi f_p}{\gamma} (t - t_0) \right) \right] \cos[2\pi f_p(t - t_0) + \nu], & t_0 - \frac{\gamma}{2f_p} \leq t \leq t_0 + \frac{\gamma}{2f_p} \text{ with } \gamma > 1 \\ 0, & \text{otherwise} \end{cases} \quad (1)$$

where A controls the amplitude of the signal, f_p is the prevailing frequency of the signal, ν is the phase of the amplitude-modulated harmonic, γ is a parameter that defines the oscillatory character of the signal, and t_0 specifies the epoch of the envelope’s peak. The pulse period T_p is defined as the inverse of the prevailing frequency f_p , that is: $T_p = 1/f_p$. Mavroeidis and Papageorgiou [12] also derived a closed-form expression for the Fourier transform $V(\omega)$ of the velocity signal provided by Equation (1) as a function of A , f_p , γ , and ν . The Fourier transform $D(\omega)$ of the corresponding displacement signal can be expressed as $D(\omega) = V(\omega)/(i\omega)$.

Empirical relationships and practical guidelines have been proposed [12–14] for the selection of the input parameters of the mathematical model of Equation (1). For interplate tectonic regimes and under the requirement of self-similarity, the pulse period T_p is related to the earthquake magnitude M_W through the following equation [12, 14]:

$$\log T_p = -2.9 + 0.5M_W \quad (2)$$

The amplitude of the near-fault velocity records has been found to be a fairly stable parameter with a value of 100 cm/s effectively representing the peak ground velocity within a few kilometers from the

fault regardless of the earthquake magnitude [12]. Attenuation relationships for peak ground velocity with rupture distance have also been proposed by [13, 14]. Parameter γ varies from a value slightly larger than 1 up to a maximum value of 3, whereas the phase angle ν ranges from 0 to 360° [12, 13]. Probability density functions for γ and ν , assuming that these two parameters are normally distributed, have also been proposed in [13].

Following Cao et al. [11], T_p is assumed to range from 0.5 to 10 s, which corresponds to M_W between 5.2 and 7.8 according to Equation (2). Parameter A is set equal to 100 cm/s for sites located within a few kilometers from the fault. The effect of γ is taken into account by considering four characteristic values: 1.0, 1.5, 2.0, and 3.0. Finally, parameter ν is set equal to 90° to ensure that the displacement offset vanishes for all synthetic motions in agreement with the waveform characteristics of pure forward directivity motions (see discussion in [11]).

3. SOIL–FOUNDATION–STRUCTURE SYSTEM

Figure 1a illustrates the soil–foundation–structure model adopted in this study (modified after [3]) to evaluate the effects of wave passage on the accidental eccentricity of symmetric, elastic buildings subjected to near-fault pulse-like ground motions. The superstructure is modeled as a uniform elastic bar of height H and radius a . The foundation is represented by a surface-supported rigid circular disc of negligible thickness and the same radius as the superstructure. Parameters m_b and m_0 denote the masses of the superstructure and the foundation, respectively, whereas the corresponding mass moments of inertia about the z axis are I_b and I_0 . In addition, J_0 represents the mass moment of inertia of the foundation about the y axis. The superstructure is characterized by uncoupled fixed-base fundamental translational and torsional frequencies ω_x and ω_θ , respectively, whereas the corresponding hysteretic damping factors are denoted by ζ_x and ζ_θ . The soil is assumed to be an elastic, homogeneous, and isotropic halfspace with shear wave velocity β , shear modulus G , Poisson's ratio σ , and density ρ_s .

As shown in Figure 1a, the excitation of the system is represented by an obliquely incident plane SH wave propagating at an angle θ with respect to the y axis (i.e. angle of incidence), whereas the particle motion is parallel to the x axis. Under this type of excitation, the response of the foundation–superstructure system can be decomposed into two parts: translation and rocking in the x – z plane (Figure 1b) and torsion about the z axis (Figure 1c). Because the superstructure and the foundation are both symmetric, the translational-rocking and torsional responses are uncoupled and thus can be studied independently. In order to model realistic building configurations and site conditions, 40 actual buildings with distinct characteristics are considered in this study. The building properties,

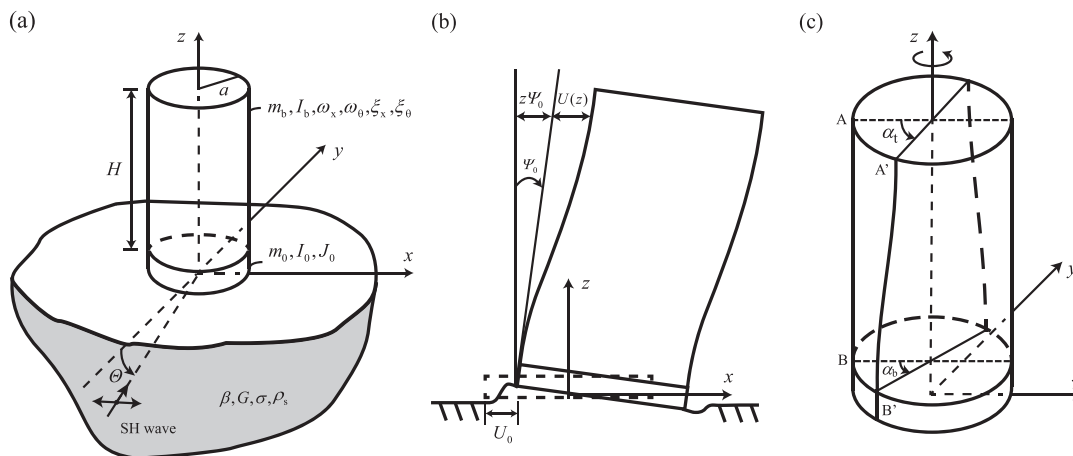


Figure 1. (a) Model of soil–foundation–structure system (modified after [3]). (b) Translational and rocking response of foundation–superstructure in x – z plane. (c) Torsional response of foundation–superstructure about z axis.

obtained from the empirical investigation of SSI effects conducted by Stewart et al. [15], have been summarized in Table 1 of Cao et al. [11] and thus are not discussed further herein for the sake of brevity.

Even though the soil–foundation–structure model considered in this study does not account for the effects of nonlinear response and foundation flexibility, it is considered to be appropriate for the following reasons: (i) the response of buildings to strong earthquake motions, although nonlinear, may be described by linear models with appropriate values of period and equivalent damping, provided that the structural yielding is not excessive and is well distributed over the structure [16]. It is clear that more realistic models that take into account the detailed building geometry and the nonlinear response are required to capture more accurately the behavior of the soil–foundation–structure system for design purposes; (ii) the near-fault pulse-like ground motions considered in this study are associated with wavelengths that are significantly greater than the size of the footprint of a reasonably-sized structure, thus implying that the foundation flexibility would not affect the structural response considerably; and (iii) the selected model provides the analytical tools to quantify the impact of variations in the input parameters of the seismic excitation and soil–foundation–structure system on structural response.

4. TRANSLATIONAL RESPONSE DUE TO SIMPLIFIED NEAR-FAULT PULSE-LIKE GROUND MOTIONS

4.1. Transfer functions

4.1.1. *Mathematical formulation.* The mathematical formulation that follows was originally developed, and preliminary results were presented by Meza-Fajardo and Papageorgiou [17]. The seismic excitation depicted in Figure 1a is represented by an obliquely incident plane SH wave of amplitude $u_{g0}/2$ and steady-state frequency ω expressed by

$$U_{gx}^i(x, y, z) = \frac{u_{g0}}{2} e^{i\omega(t - \frac{y}{\beta} \cos\theta - \frac{z}{\beta} \sin\theta)} \tag{3}$$

In the absence of the rigid foundation, the incident wave of Equation (3) and its total reflection on the free surface combine to generate the free-field motion

$$U_{gx}^{i+r}(x, y, z) = u_{g0} e^{i\omega(t - \frac{y}{\beta} \cos\theta)} \cos\left(\frac{\omega z}{\beta} \sin\theta\right) \tag{4}$$

Figure 1b illustrates the response of the foundation–superstructure system in the x – z plane under the action of the incident wave of Equation (3). The foundation response consists of a translational horizontal component U_0 along the x axis and a rocking component Ψ_0 about the y axis, both defined with respect to the position of the foundation prior the occurrence of seismic disturbances. On the other hand, the response of the superstructure is described by a horizontal translation $U(z)$ at level z relative to its base, which is in addition to the horizontal translation $z\Psi_0$ caused by foundation rocking.

The response of the foundation, which consists of horizontal translation U_0 and rocking Ψ_0 , may conveniently be written in the form of (e.g. [18])

$$\begin{Bmatrix} U_0 \\ a\Psi_0 \end{Bmatrix} = \begin{Bmatrix} U_0^* \\ a\Psi_0^* \end{Bmatrix} + \begin{Bmatrix} U_s \\ a\Psi_s \end{Bmatrix} \tag{5}$$

where U_0^* and Ψ_0^* are the foundation input motions obtained by evaluating the response of the rigid massless foundation to the incident SH wave in the absence of the superstructure, and U_s and Ψ_s are additional motions of the foundation associated with the deformation of the soil caused by the force and moment that the foundation exerts on the soil. For conciseness, the time factor $e^{i\omega t}$ is omitted

both from Equation (5) and from the mathematical formulation presented in the remainder of this section.

The translational component U_0^* of the foundation input motion for the soil–foundation–structure system shown in Figure 1a can be calculated by multiplying a frequency-dependent function S_{xx} by the free-field motion of Equation (4) evaluated at $(y,z) = (0,0)$:

$$U_0^* = S_{xx}u_{g0} \quad (6)$$

Luco and Mita [19] have provided values of S_{xx} in tabular form as a function of the dimensionless frequency $a_0 = a\omega/\beta$ for $\beta/c_{app} = 0.1, 0.2, 0.3, 0.4, 0.5$ and $\sigma = 0.33, 0.45$, where c_{app} is the wave apparent velocity (i.e. $c_{app} = \beta/\cos\Theta$). These β/c_{app} values correspond to angles of incidence Θ ranging from 60.0° to 84.3° , which are deemed sufficient to characterize the incident angles of shear waves in the near-fault region (e.g. [11, 20]). In addition, the rocking component Ψ_0^* of the foundation input motion has been found to be very small for flat foundations excited by SH waves and can be neglected for all practical purposes [21].

On the other hand, the additional motions U_s and Ψ_s are related to the force V_s and moment M_s that the foundation exerts on the soil as follows

$$\begin{Bmatrix} V_s \\ \left(\frac{M_s}{a}\right) \end{Bmatrix} = \mathbf{K}(\omega) \begin{Bmatrix} U_s \\ a\Psi_s \end{Bmatrix} = Ga \begin{bmatrix} K_{HH} & K_{HM} \\ K_{MH} & K_{MM} \end{bmatrix} \begin{Bmatrix} U_s \\ a\Psi_s \end{Bmatrix} \quad (7)$$

where $\mathbf{K}(\omega)$ is the frequency-dependent impedance matrix. The terms K_{HH} , $K_{HM} = K_{MH}$, and K_{MM} correspond to the normalized horizontal, coupling, and rocking impedance functions, for which tabular data, as a function of $a_0 = a\omega/\beta$ for $\sigma = 0.33, 0.45$, have also been provided by [19].

Assuming that the superstructure is modeled as a uniform shear beam, an approach that has widely been used by earthquake engineers to study the seismic response of buildings (despite its limitation of only accounting for shear deformations), the equation of motion under harmonic excitation of foundation translation U_0 and rocking Ψ_0 is given by

$$k(1 + 2i\zeta_x) \frac{d^2U(z)}{dz^2} + m\omega^2 U(z) = -m\omega^2 U_0 - m\omega^2 z\Psi_0, \quad 0 \leq z \leq H \quad (8)$$

where $U(z)$ is the translational response, k is the shear stiffness, m is the mass per unit length, and ζ_x is the hysteretic damping factor for translational vibrations. The fundamental translational frequency ω_x of the fixed-base superstructure is

$$\omega_x = \frac{\pi}{2H} \sqrt{\frac{k}{m}} \quad (9)$$

The translational response $U(z)$ must satisfy the following boundary conditions

$$U(z=0) = 0, \quad V(z=H) = k(1 + 2i\zeta_x) \frac{dU(z)}{dz} \Big|_{z=H} = 0 \quad (10a-b)$$

where $V(z)$ is the shear force at level z and H is the height of the structure. The solution of Equation (8), subject to the boundary conditions expressed by Equation (10a–b), is

$$U(z) = [\cos(k_{bx}z) + \tan(k_{bx}H) \sin(k_{bx}z) - 1]U_0 + \left[\frac{\sin(k_{bx}z)}{k_{bx} \cos(k_{bx}H)} - z \right] \Psi_0 \quad (11)$$

where

$$k_{bx} = \omega \sqrt{\frac{m}{k(1 + 2i\zeta_x)}} = \frac{\pi}{2H} \left(\frac{\omega}{\omega_x}\right) \frac{1}{\sqrt{1 + 2i\zeta_x}} \tag{12}$$

The base shear V_b and base moment M_b that the superstructure exerts on the foundation may then be evaluated as

$$V_b = k(1 + 2i\zeta_x) \frac{dU(z)}{dz} \Big|_{z=0} = \left(\frac{m\omega^2}{k_{bx}}\right) \left\{ \tan(k_{bx}H)U_0 + \left[\frac{\sec(k_{bx}H) - 1}{k_{bx}}\right] \Psi_0 \right\} \tag{13}$$

$$M_b = \int_0^H z m \omega^2 [U(z) + U_0 + z\Psi_0] dz = \left(\frac{m\omega^2}{k_{bx}}\right) \left\{ \left[\frac{\sec(k_{bx}H) - 1}{k_{bx}}\right] U_0 + \left(\frac{1}{k_{bx}}\right) \left[\frac{\tan(k_{bx}H)}{k_{bx}} - H\right] \Psi_0 \right\} \tag{14}$$

Equations (13) and (14) can properly be normalized and expressed in matrix form as

$$\begin{Bmatrix} V_b \\ \left(\frac{M_b}{a}\right) \end{Bmatrix} = \omega^2 \left(\frac{m_b}{k_{bx}H}\right) \left(\frac{H}{a}\right) \begin{bmatrix} \left(\frac{H}{a}\right)^{-1} \tan(k_{bx}H) & \frac{\sec(k_{bx}H) - 1}{k_{bx}H} \\ \frac{\sec(k_{bx}H) - 1}{k_{bx}H} & \left(\frac{H}{a}\right) \left[\frac{\tan(k_{bx}H) - k_{bx}H}{(k_{bx}H)^2}\right] \end{bmatrix} \begin{Bmatrix} U_0 \\ a\Psi_0 \end{Bmatrix} \tag{15}$$

where $m_b = mH$ is the mass of the superstructure.

By considering the coupling of superstructure and soil through the foundation, the dynamic force and moment equilibrium equations for the foundation can be written in matrix form as

$$-\omega^2 \begin{bmatrix} m_0 & 0 \\ 0 & \left(\frac{J_0}{a^2}\right) \end{bmatrix} \begin{Bmatrix} U_0 \\ a\Psi_0 \end{Bmatrix} = \begin{Bmatrix} V_b \\ \left(\frac{M_b}{a}\right) \end{Bmatrix} - \begin{Bmatrix} V_s \\ \left(\frac{M_s}{a}\right) \end{Bmatrix} \tag{16}$$

By substituting Equations (7) and (15) into Equation (16) and then combining with Equation (5), the response of the foundation (U_0 and Ψ_0) can be expressed in terms of the foundation input motions (U_0^* and Ψ_0^*) as

$$\begin{Bmatrix} U_0 \\ a\Psi_0 \end{Bmatrix} = \left(\mathbf{I}_2 - \frac{\omega^2}{Ga} \begin{bmatrix} K_{HH} & K_{HM} \\ K_{MH} & K_{MM} \end{bmatrix} \right)^{-1} \left(\begin{bmatrix} m_0 & 0 \\ 0 & \left(\frac{J_0}{a^2}\right) \end{bmatrix} + \left(\frac{m_b}{k_{bx}H}\right) \left(\frac{H}{a}\right) \begin{bmatrix} \left(\frac{H}{a}\right)^{-1} \tan(k_{bx}H) & \frac{\sec(k_{bx}H) - 1}{k_{bx}H} \\ \frac{\sec(k_{bx}H) - 1}{k_{bx}H} & \left(\frac{H}{a}\right) \left[\frac{\tan(k_{bx}H) - k_{bx}H}{(k_{bx}H)^2}\right] \end{bmatrix} \right)^{-1} \begin{Bmatrix} U_0^* \\ a\Psi_0^* \end{Bmatrix} \tag{17}$$

By using the relationship between shear wave velocity β and shear modulus G (i.e. $\beta = \sqrt{G/\rho_s}$) along with the definition of the dimensionless frequency a_0 (i.e. $a_0 = a\omega/\beta$), the expression $\omega^2/(Ga)$ appearing in Equation (17) may alternatively be written as $a_0^2/(\rho_s a^3)$. By substituting Equation (6) into Equation (17) and setting $\Psi_0^* = 0$ (based on the preceding discussion), the response of the foundation (U_0 and Ψ_0) can be expressed in terms of the free-field motion (u_{g0}) as

$$\begin{Bmatrix} U_0 \\ a\Psi_0 \end{Bmatrix} = \left(\mathbf{I}_2 - \left(\alpha_x \frac{\omega}{\omega_x}\right)^2 \begin{bmatrix} K_{HH} & K_{HM} \\ K_{MH} & K_{MM} \end{bmatrix} \right)^{-1} \left(\begin{bmatrix} \left(\frac{m_0}{m_s}\right) & 0 \\ 0 & \left(\frac{J_0}{J_s}\right) \end{bmatrix} + \left(\frac{m_b}{k_{bx}H}\right) \left(\frac{H}{a}\right) \begin{bmatrix} \left(\frac{H}{a}\right)^{-1} \tan(k_{bx}H) & \frac{\sec(k_{bx}H) - 1}{k_{bx}H} \\ \frac{\sec(k_{bx}H) - 1}{k_{bx}H} & \left(\frac{H}{a}\right) \left[\frac{\tan(k_{bx}H) - k_{bx}H}{(k_{bx}H)^2}\right] \end{bmatrix} \right)^{-1} \begin{Bmatrix} S_{xx}u_{g0} \\ 0 \end{Bmatrix} \tag{18}$$

where

$$\alpha_x = a\omega_x/\beta = a_0\omega_x/\omega, \quad m_s = \rho_s a^3, \quad J_s = m_s a^2 \tag{19a-c}$$

In Equations (18) and (19), a_x is the relative stiffness parameter for translational vibrations, and m_s and J_s are the ‘soil mass’ and ‘soil moment of inertia’ introduced to conveniently write Equation (18) in terms of dimensionless parameters.

Once the translational and rocking components of the foundation response are obtained from Equation (18), the translational response of the superstructure at any level z can readily be calculated using Equation (11). In particular, the translational response at the top of the superstructure U_H [i.e. $U(z)$ at $z = H$] is provided by the following equation

$$U_H = [\cos(k_{bx}H) + \tan(k_{bx}H) \sin(k_{bx}H) - 1]U_0 + \left[\frac{\tan(k_{bx}H)}{k_{bx}H} - 1 \right] \left(\frac{H}{a} \right) (a\Psi_0) \quad (20)$$

Equations (18) and (20) indicate that the frequency domain responses of the foundation (U_0 and Ψ_0) and top of the superstructure (U_H), also known as transfer functions, may be described in terms of the following dimensionless parameters: normalized frequency ω/ω_x , relative stiffness parameter a_x for translational vibrations, ratio of building height to foundation radius H/a (also known as slenderness ratio), mass ratios m_b/m_s and m_0/m_s , moment-of-inertia ratio J_0/J_s , hysteretic damping factor ζ_x for translational vibrations, function S_{xx} , and normalized impedance functions K_{HH} , K_{HM} , and K_{MM} . Note that parameter $k_{bx}H$, appearing in Equations (18) and (20), is also a dimensionless parameter which depends on ω/ω_x , and ζ_x [see Equation (12)].

4.1.2. Input parameters. In Table 1 of Cao et al. [11], the building height H , the foundation radius a , the fixed-base fundamental translational period $T_x = 2\pi/\omega_x$, and the soil shear wave velocity β are provided for 40 buildings. Using this information, the slenderness ratio H/a and the relative stiffness parameter $a_x = a\omega_x/\beta$ can readily be calculated for each building. The H/a values range from 0.3 to 6.9 with the larger values typically corresponding to tall buildings, whereas the a_x values are between 0.1 and 2.3; it is only Building A1 on soft soil (i.e. small β) and Building A17 with a large foundation radius that are characterized by a_x values of 3.4 and 4.4, respectively.

The mass ratios m_b/m_s and m_0/m_s and the moment-of-inertia ratio J_0/J_s are determined through the following steps. The mass of the superstructure m_b may be estimated from

$$m_b = \rho_b H A \quad (21)$$

where ρ_b , H , and $A = \pi a^2$ are the mass density, height, and floor area of the superstructure. The mass ratio m_b/m_s may be determined by combining Equations (19b) and (21) resulting in $m_b/m_s = \pi(\rho_b/\rho_s)(H/a)$. If $\delta_m = m_0/m_b$ denotes the foundation-to-superstructure mass ratio, m_0/m_s may be obtained by multiplying the mass ratio m_b/m_s by δ_m . Considering that the foundation is modeled as a circular disc, its moment of inertia about the y axis is calculated from $J_0 = m_0 a^2/4$. By combining the latter equation with Equation (19c), it follows that $J_0/J_s = m_0/(4m_s)$. Therefore, dimensionless parameters m_b/m_s , m_0/m_s , and J_0/J_s may be determined for each building from the slenderness ratio H/a and typical values of soil density ρ_s , mass density of the superstructure ρ_b , and foundation-to-superstructure mass ratio δ_m . In this study, it is assumed that $\rho_s = 1.95 \text{ Mg/m}^3$, $\rho_b = 250 \text{ kg/m}^3$, and $\delta_m = 0.2$, consistent with typical properties of the soil–foundation–structure system (see discussion in [11]). Finally, the hysteretic damping factor ζ_x for translational vibrations is set equal to 4%.

4.1.3. Parametric analysis. The characteristics of the transfer function of the translational response at the top of the superstructure, expressed by Equation (20), are investigated through a parametric analysis. Based on the discussion in Section 4.1.2, the selected values of the relative stiffness parameter and slenderness ratio are $a_x = 0.1, 1.5, 3.0$ and $H/a = 0.3, 1.0, 3.0, 6.0$. Note that large values of a_x typically represent very stiff buildings or very soft soils, whereas large values of H/a correspond to tall slender buildings. Parameters m_b/m_s , m_0/m_s , and J_0/J_s are then calculated using the selected values of H/a along with the fixed values of ρ_s , ρ_b , and δ_m listed in Section 4.1.2. Subsequently, U_0 and Ψ_0 are computed from Equation (18) for the selected values of a_x and the tabulated values of S_{xx} , K_{HH} , K_{HM} , and K_{MM} provided by [19] for $\beta/c_{app} = 0.1, 0.3$, and 0.5 . Larger values of β/c_{app} correspond to incident SH waves traveling in a more horizontal direction. Finally, U_H is calculated from Equation (20). It should be noted that the calculations for Poisson’s

ratios $\sigma = 0.33$ and 0.45 produce very similar results; thus, σ is fixed to 0.33 for the analysis results presented in the remainder of this article.

Figure 2 illustrates the variation of the modulus of translational response $|U_H/u_{g0}|$ at the top of the superstructure as a function of the normalized frequency ω/ω_x for distinct values of a_x , H/a , and β/c_{app} . Inspection of Figure 2 reveals that the amplitude of the first peak response and the corresponding normalized resonance frequency decrease as a_x increases from 0.1 to 3.0 for a prescribed value of H/a . This observation, which is more pronounced for larger values of H/a (i.e. tall slender buildings), has also been reported in previous studies (e.g. [22, 23]). On the other hand, non-vertical SH waves tend to reduce the response for higher frequencies (e.g. $\omega/\omega_x > 1.0$), especially for smaller values of H/a (e.g. $H/a < 1.0$) and larger values of a_x (e.g. $a_x > 1.5$). This reduction in response is more pronounced with increasing β/c_{app} . It is also worth mentioning that the amplitude of the first peak response is generally insensitive to the variation of β/c_{app} . Finally, the variation of H/a appears to have negligible effects on the response when a_x is very small (e.g. $a_x = 0.1$). Note that a very small value of a_x implies that the soil is much stiffer than the superstructure, and thus the rocking response of the foundation is expected to be small. Therefore, the slenderness ratio H/a , which is associated with the response of the superstructure due to foundation rocking, is not important for small a_x values.

4.2. Translational response

In this section, a detailed analysis is performed to examine the translational response of all 40 buildings considered in this study under the action of simplified near-fault pulse-like ground motions. The seismic excitation input is described using the mathematical model proposed by Mavroeidis and Papageorgiou [12] (see Section 2). The translational displacement at the top of the superstructure (i.e. termed ‘translational displacement’ for simplicity) is first calculated in the frequency domain by multiplying the transfer function $U_H(\omega)$ of Equation (20) by the Fourier transform $D(\omega)$ of the simplified ground displacement (see Section 2). The translational response in the time domain is then obtained by applying the inverse fast Fourier transform. The response quantity of interest is the maximum absolute value of the translational displacement time history.

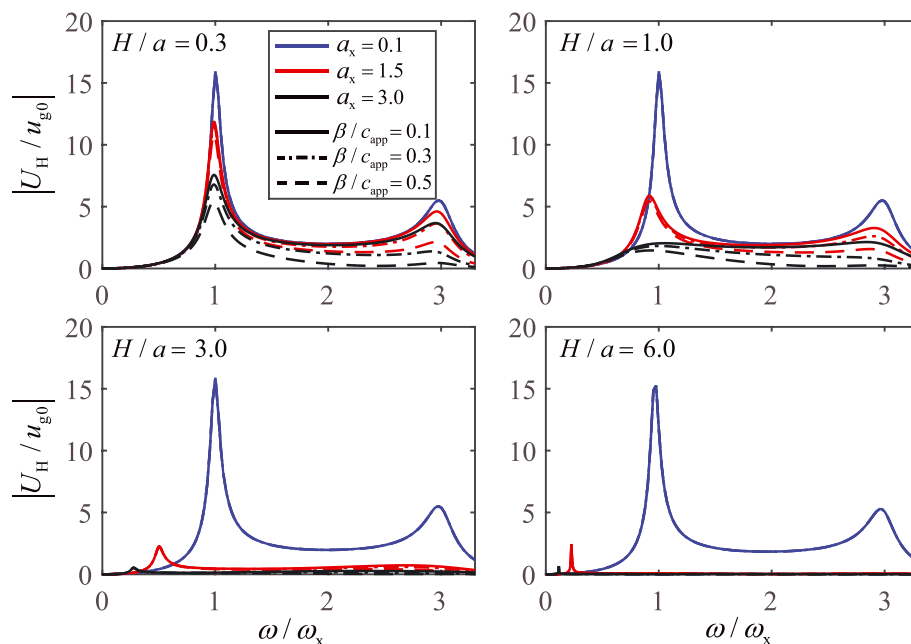


Figure 2. Modulus of the translational response $|U_H/u_{g0}|$ at the top of the superstructure as a function of the normalized frequency ω/ω_x for $a_x = 0.1, 1.5, 3.0$, $H/a = 0.3, 1.0, 3.0, 6.0$, and $\beta/c_{app} = 0.1, 0.3, 0.5$. [Colour figure can be viewed at wileyonlinelibrary.com]

4.2.1. Effect of ground motion parameters. Three buildings with short, intermediate, and long periods are selected to examine the effect of ground motion parameters on translational response: Building A10 (3 stories, $H = 14.4$ m, $a = 22.9$ m, $T_x = 0.28$ s and $\beta = 234.1$ m/s), Building A36 (6 stories, $H = 23.1$ m, $a = 15.2$ m, $T_x = 1.07$ s and $\beta = 362.1$ m/s), and Building A28 (19 stories, $H = 95.8$ m, $a = 28.0$ m, $T_x = 3.45$ s and $\beta = 298.7$ m/s). Figure 3 presents the maximum translational displacement of the three buildings as a function of T_p/T_x for different values of γ , whereas β/c_{app} is considered to be 0.1. Because the T_p values considered in this study range from 0.5 to 10 s (corresponding to M_W 5.2–7.8), the effective range of T_p/T_x over which Figure 3 is plotted differs for each of the three buildings.

The peak of the maximum translational displacement is attained when T_p/T_x approaches a value slightly larger than one (see Buildings A36 and A28), indicating that resonance occurs when the pulse period approaches the fundamental translational period of the building. This observation is consistent with results reported previously regarding the resonance response of single-degree-of-freedom (SDOF) systems subjected to near-fault pulse-like ground motions (e.g. [24, 25]). In addition, as γ increases from 1 to 3, the peak of the maximum translational displacement increases by a factor of ~ 2 , and the shape of the response curve changes gradually from ‘flattened’ to ‘peaked’. On the other hand, Building A10 is not subjected to resonance due to the range of T_p/T_x values considered in this study, thus resulting in significantly smaller response. Note that for generating Figure 3, parameter β/c_{app} is set equal to 0.1. Additional simulations for $\beta/c_{app} = 0.2, 0.3, 0.4, 0.5$ reveal that β/c_{app} exerts an insignificant effect on the maximum translational displacement. This can be attributed to the fact that buildings, under the action of simplified long-period pulses, vibrate primarily in their fundamental mode, and the amplitude of the transfer function at the fundamental mode is generally insensitive to β/c_{app} (see Section 4.1.3 and Figure 2).

To further demonstrate the dominant effect of the fundamental mode, a similar parametric analysis was conducted for all 40 buildings with the response quantity of interest now being the overall maximum translational displacement between any point along the height of the building and its base. The analysis results (not shown here) suggested that the maximum translational displacement occurs at the top of the building for the vast majority of cases. It is only for a few long-period buildings (e.g. $T_x > 3.0$ s) with $T_p/T_x < 0.4$ that the maximum displacement at the top may slightly underestimate the overall maximum displacement along the height of the building due to higher mode effects.

4.2.2. Effect of shear wave velocity. In order to investigate the effect of shear wave velocity on translational response, four representative values of β are selected, corresponding to the National Earthquake Hazards Reduction Program Site Classes B, C, D, and E [26]. Figure 4a presents the

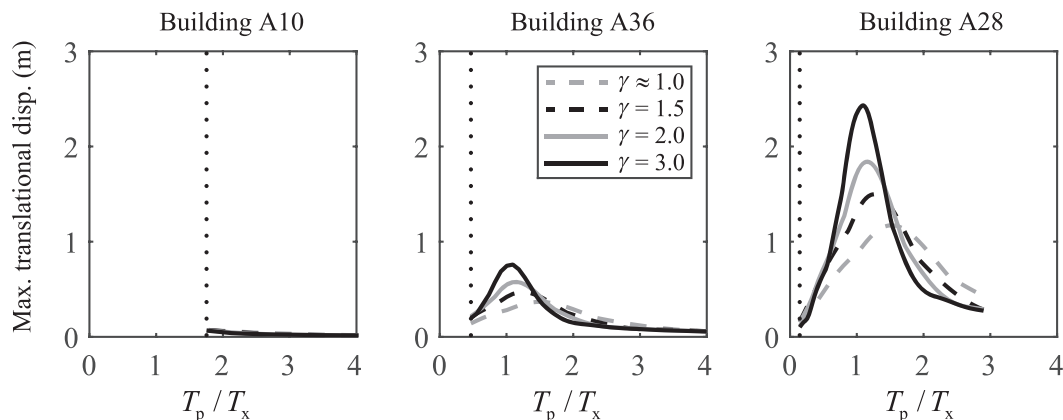


Figure 3. Maximum translational displacement at the top of Buildings A10, A36, and A28 vs. T_p/T_x for $\gamma = 1.0, 1.5, 2.0, 3.0$ and $\beta/c_{app} = 0.1$. The dotted vertical line specifies the lower limit of the effective range of T_p/T_x for each building.

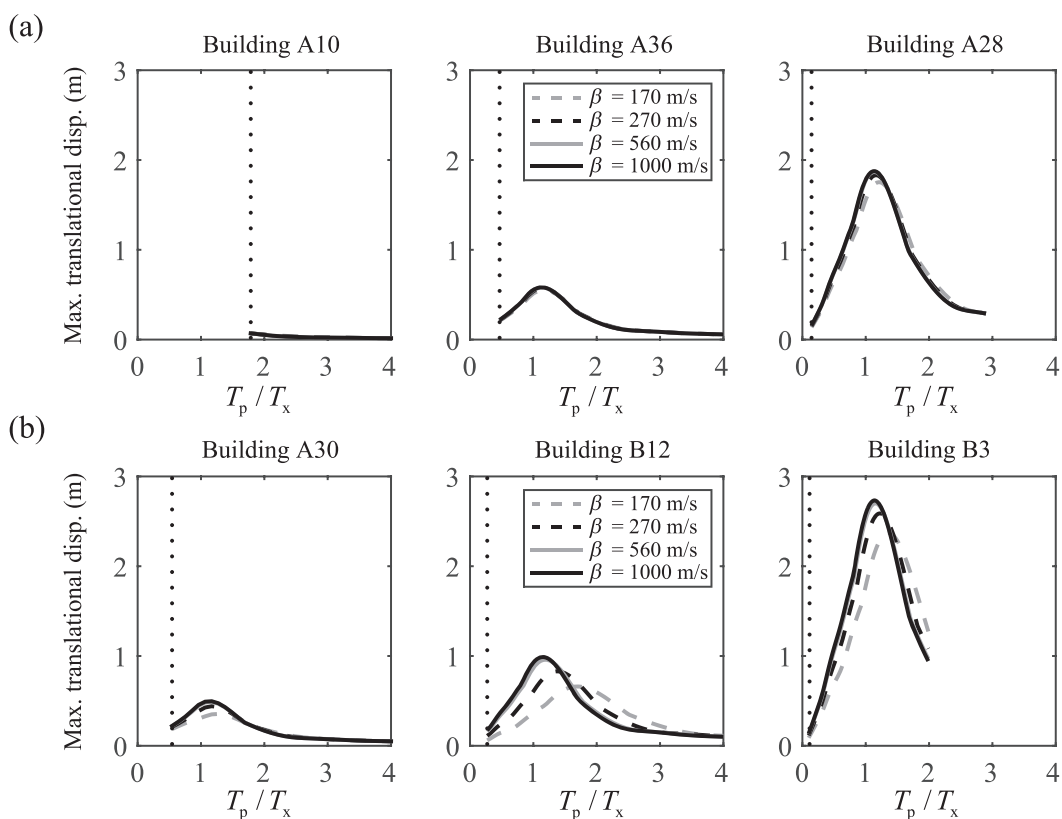


Figure 4. (a) Maximum translational displacement at the top of Buildings A10, A36, and A28 vs. T_p/T_x for $\beta = 170, 270, 560, 1000$ m/s, $\gamma = 2.0$ and $\beta/c_{app} = 0.1$. (b) Same parametric analysis for Buildings A30, B12, and B3. The dotted vertical line specifies the lower limit of the effective range of T_p/T_x for each building.

maximum translational displacement of the three buildings shown in Figure 3 as a function of T_p/T_x for $\beta = 170, 270, 560, 1000$ m/s, $\gamma = 2.0$, and $\beta/c_{app} = 0.1$. It appears that the maximum translational displacements of Buildings A10 and A36 are insensitive to β , whereas the response curve for Building A28 is only slightly affected by β .

Figure 4b presents parametric analysis results for three additional buildings exhibiting more noticeable effects of β : Building A30 (6 stories, $H = 34.0$ m, $a = 57.6$ m, $T_x = 0.92$ s), Building B12 (32 stories, $H = 130.6$ m, $a = 28.3$ m, $T_x = 1.84$ s), and Building B3 (47 stories, $H = 180.3$ m, $a = 26.2$ m, $T_x = 5.03$ s). For Buildings A30, B12, and B3, as β decreases from 1000 to 170 m/s, the peak response decreases, and the corresponding value of T_p/T_x shifts towards larger values. This is consistent with findings reported by Veletsos and Meek [23] for building–foundation systems subjected to pulse-type excitations. This observation, which is not always evident in the response curves of buildings (e.g. Building A36 in Figure 4a), requires an explanation. A decrease in β translates into an increase in $a_x = a\omega_x/\beta$, which in turn implies that the amplitude of the first peak response of the transfer function and the corresponding value of ω/ω_x both decrease (see Section 4.1.3 and Figure 2). These effects on transfer function tend to decrease the peak value of the maximum translational response and increase the corresponding value of T_p/T_x as shown in Figure 4b. However, the reduction in the amplitude of the peak response also depends on the corresponding value of T_p , which affects the Fourier transform $D(\omega)$ of the seismic excitation input [12, 11]. In comparison with Buildings A10, A36, and A28 (Figure 4a), the more pronounced effect of β on the response of Buildings A30, B12, and B3 (Figure 4b) is attributed to the particular values of H/a and a_x , which directly affects the respective transfer functions (Figure 2). Finally, it should be noted that additional simulations for $\beta/c_{app} = 0.2, 0.3, 0.4, 0.5$ reveal that parameter β/c_{app} has a

negligible effect on the analysis results shown in Figure 4 because of the dominance of the fundamental mode response.

4.2.3. Effect of building parameters. Figure 5 shows the response curves of all 40 buildings as a function of T_p/T_x and T_x for $\beta = 170, 270, 560, 1000$ m/s, $\gamma = 2.0$, and $\beta/c_{app} = 0.1$. Inspection of the figure reveals that all response curves have a similar shape and the peak value of the maximum translational displacement occurs at $T_p/T_x \approx 1.1$. This observation is in agreement with findings reported previously for elastic SDOF systems subjected to near-fault pulse-like ground motions (e.g. [24, 25]). The similarity between results obtained from the shear beam model and the SDOF system can be attributed to the fact that the shear beam model, under the action of simplified long-period pulses, vibrates primarily in its fundamental mode. Figure 5 also illustrates that the maximum translational displacement for a fixed T_p/T_x value tends to increase with increasing values of T_x . It is worth mentioning that, for small values of β (i.e. 170 and 270 m/s) and depending on the values of H/a and a_x , the peak displacement response of certain buildings may occur at T_p/T_x values greater than 1.1 due to the effect of shear wave velocity on maximum translational displacement (see Section 4.2.2 and Figure 4). Finally, it should be noted that the variation of β/c_{app} from 0.1 to 0.5 has an insignificant effect on the response curves of all 40 buildings shown in Figure 5.

Based on the parametric analysis results presented in Sections 4.2.1–4.2.3, it appears that the translational response of buildings to near-fault pulse-like ground motions is primarily affected by γ , T_p , and T_x , whereas β may also have measurable effects depending on parameters a_x and H/a .

5. TORSIONAL RESPONSE DUE TO SIMPLIFIED NEAR-FAULT PULSE-LIKE GROUND MOTIONS

The torsional response in the frequency domain of the soil–foundation–structure system shown in Figure 1a subjected to an obliquely incident plane SH wave has been derived analytically by Luco [3]. For the sake of brevity, only the final solution is presented in this section.

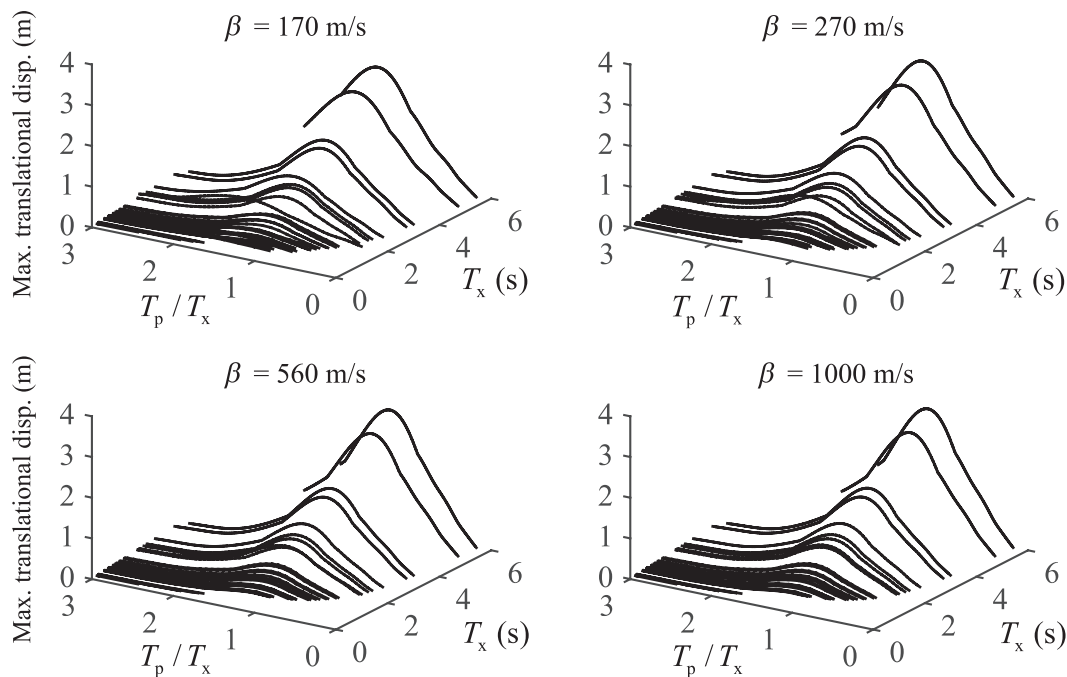


Figure 5. Maximum translational displacement at the top of all 40 buildings vs. T_p/T_x and T_x for $\beta = 170, 270, 560, 1000$ m/s, $\gamma = 2.0$ and $\beta/c_{app} = 0.1$.

The base twist α_b of the superstructure (see Figure 1c) is provided by

$$\frac{\alpha\alpha_b(\omega)}{u_{g0}} = \frac{S\left(a_0 \frac{\omega}{\omega_0}, \Theta\right)}{1 - \frac{\pi}{20} \left(a_0 \frac{\omega}{\omega_0}\right)^2 \left\{ \frac{I_b}{I_s} + \frac{I_0}{I_s} \left[\frac{\tan(k_{b0}H)}{k_{b0}H} \right] \right\} \frac{K_{TT}(0)}{K_{TT}\left(a_0 \frac{\omega}{\omega_0}\right)}} \tag{22}$$

where

$$S\left(a_0 \frac{\omega}{\omega_0}, \Theta\right) = a \alpha^* / u_{g0}, \quad a_0 = a\omega_0/\beta = a_0\omega_0/\omega, \quad k_{b0}H = \frac{\pi}{2} \left(\frac{\omega}{\omega_0}\right) \frac{1}{\sqrt{1 + 2i\zeta_0^2}} \tag{23a-c}$$

$$I_s = \frac{4\pi}{15} \rho_s a^5, \quad I_b = \frac{1}{2} m_b a^2, \quad I_0 = \frac{1}{2} m_0 a^2 \tag{23d-f}$$

$$\alpha^* = \left(8iGa^3 a_0 \cos\Theta \int_0^1 \theta_s(t) dt / K_{TT}(a_0)\right) u_{g0}/a, \quad K_{TT}(a_0) = 16Ga^3 \int_0^1 \theta_R(t) dt \tag{23g-h}$$

Note that ω_0 is the fundamental torsional frequency, ζ_0 is the hysteretic damping factor for torsional vibrations, a_0 is the relative stiffness parameter for torsional vibrations, and θ_R and θ_S are functions associated with the solution of the Fredholm integral equations.

Once the base twist α_b has been obtained from Equation (22), the top twist α_t (see Figure 1c) is calculated by

$$\alpha_t(\omega) = \alpha_b(\omega) \sec(k_{b0}H) \tag{24}$$

and the relative twist α_r between the top and the base of the superstructure is defined as

$$\alpha_r(\omega) = \alpha_t(\omega) - \alpha_b(\omega) \tag{25}$$

In summary, the transfer function of the relative twist of the superstructure expressed by Equation (25) is described in terms of the following dimensionless parameters: normalized frequency ω/ω_0 , relative stiffness parameter a_0 for torsional vibrations, ratios of moments of inertia I_b/I_s and I_0/I_s , hysteretic damping factor ζ_0 for torsional vibrations, and angle of incidence Θ .

The uncoupled torsional-to-translational frequency ratio is denoted by $\Omega = \omega_0/\omega_x = T_x/T_0$, with $\Omega \geq 1$ implying a torsionally stiff system and $\Omega < 1$ implying a torsionally flexible system. A torsionally stiff system normally has stiffer members located towards the periphery of the structure, whereas a torsionally flexible system has stiffer members located towards its center. Several studies in the published literature have recommended representative values of Ω . For instance, Chandler and Hutchinson [27] suggested that most buildings have a frequency ratio Ω in the range of 0.5–1.5 and values below 0.5 are very unlikely to occur. Based on analysis results for an idealized one-storey building consisting of a rigid deck supported on frames or walls, Riddell and Santa-Maria [28] concluded that the maximum feasible value of Ω for a circular slab is equal to 2. In addition, full-scale data from artificial and natural vibrations have indicated that the frequency ratio Ω may vary between 0.8 and 2.0 with a mean value of ~1.3 (e.g. [29, 30]).

Because no information is available about the fundamental torsional period T_0 of the 40 buildings, the frequency ratio Ω is introduced as a free parameter to determine T_0 from T_x . For the parametric analysis presented in this study, the frequency ratio Ω is assumed to vary between 0.5 and 2.0, yet one should keep in mind that torsionally stiff systems ($\Omega \geq 1$) are more common in design practice. Once the frequency ratio Ω is selected, the fundamental torsional period T_0 and the relative stiffness parameter a_0 for torsional vibrations may be calculated for each building using the fundamental translational period T_x . In addition, the ratio of moments of inertia I_b/I_s can be determined by combining Equations (21) and (23d–e) resulting in $I_b/I_s = 1.875(\rho_b/\rho_s)(H/a)$, whereas parameter I_0/I_s may be obtained by multiplying I_b/I_s by the foundation-to-superstructure mass ratio δ_m . Subsequently, using the values of ρ_s , ρ_b , and δ_m specified in Section 4.1.2, I_b/I_s and I_0/I_s can readily

be calculated for all buildings. The hysteretic damping ratios for torsional and translational vibrations are assumed to be equal (i.e. $\zeta_\theta = \zeta_x = 4\%$). Finally, the angle of incidence θ is determined by considering typical values of the wave apparent velocity c_{app} and the shear wave velocity β (i.e. $\cos\theta = \beta/c_{app}$). Using empirical and numerical approaches, previous studies have suggested that c_{app} values of body waves in the near-fault region range between 2.0 and 3.8 km/s [4, 31, 32]. Moreover, the torsional response due to wave passage effects in the near-fault region has been found to increase for smaller values of c_{app} [4, 11]. In this study, the wave apparent velocity c_{app} is set equal to 2.0 km/s to obtain the most critical torsional response.

The interested reader is referred to Cao et al. [11] for a comprehensive parametric analysis of the transfer function of the relative twist expressed by Equation (25) and of the torsional response of the soil–foundation–structure system subjected to near-fault pulse-like ground motions. The present study further evaluates the increase in building displacements due to the torsional response arising from wave passage effects by means of accidental eccentricity.

6. EVALUATION OF ACCIDENTAL ECCENTRICITY

According to De la Llera and Chopra [7], the design accidental eccentricity arising from base rotations may be determined in such a way that, when used in conjunction with the equivalent static lateral forces, the increase in building displacement is identical to that computed from response history analysis. Based on analysis results from idealized single-story systems, De la Llera and Chopra [7] derived mathematical expressions for the accidental eccentricity of symmetric- and asymmetric-plan buildings. Because the soil–foundation–structure system considered in this study primarily vibrates in its fundamental mode, the formulation proposed in [7] is adopted to estimate the accidental eccentricity arising from base torsional motions due to wave passage effects.

Assuming that $u_x(t)$ denotes the translational displacement at the top of the superstructure and $u_\theta(t)$ represents the relative twist between the top and the base of the superstructure, the normalized response at $y = \pm r$ is defined as

$$(\tilde{u}_{\pm r})_0 = \frac{\max|u_x(t) \mp ru_\theta(t)|}{\max|u_x(t)|} \quad (26)$$

where r is the radius of gyration of the system plan about a vertical axis passing through the center of mass. For the symmetric cylindrical model shown in Figure 1, this vertical axis coincides with the z axis, and the radius of gyration is equal to $a/\sqrt{2}$. Note that quantity $ru_\theta(t)$ may be interpreted as the tangential displacement calculated at distance r along the y axis arising from base torsional motions due to wave passage effects. The normalized response \tilde{u}_0 , defined as the larger value of $(\tilde{u}_{+r})_0$ and $(\tilde{u}_{-r})_0$, provides a measure of the amplification in translational response due to the presence of torsional vibrations. For symmetric buildings with a circular floor plan, the normalized accidental eccentricity $e_a/2a$ is provided by

$$\frac{e_a}{2a} = \frac{\sqrt{2}}{4} (\tilde{u}_0 - 1) \Omega^2 \quad (27)$$

6.1. Parametric analysis

Following the selection of input parameters presented in Sections 2, 4, and 5, the translational and torsional components of the building response due to near-fault pulse-like motions are calculated for all 40 buildings. Four characteristic values of β (i.e. 170, 270, 560, 1000 m/s) are considered along with a fixed value of $c_{app} = 2.0$ km/s (see Section 5), resulting in $\beta/c_{app} = 0.085, 0.135, 0.280, 0.500$. The frequency-dependent function S_{xx} is evaluated by interpolating the tabular data provided by Luco and Mita [19] at the considered values of β/c_{app} . Once the translational and torsional components of the building response have been computed, the normalized response and the normalized accidental eccentricity are evaluated using Equations (26) and (27).

6.1.1. *Effect of frequency ratio and pulse period.* Figure 6a and b shows, respectively, the maximum translational displacement ($\max|u_x(t)|$) and the maximum displacement due to torsional vibrations ($\max|ru_\theta(t)|$) as a function of Ω and T_p/T_x for Buildings A10, A36, and A28. Note that $\max|u_x(t)|$ is significantly larger than $\max|ru_\theta(t)|$ (even for Building A10), implying that the normalized response \tilde{u}_0 occurs at a time instant t' that coincides, for all practical purposes, with the time of $\max|u_x(t)|$. Figure 6c illustrates the displacement amplitude due to torsional vibrations at t' ($|ru_\theta(t')|$), whereas Figure 6d and e presents the normalized response \tilde{u}_0 and the normalized accidental eccentricity $e_a/2a$. In generating Figure 6, it was assumed that $\beta = 270$ m/s and $\gamma = 2.0$. With reference to Figure 6, the following observations are made:

- For Building A10 ($T_x = 0.28$ s), a value of $\Omega = 0.5$ implies that $T_\theta = 0.56$ s, which is close to the lower bound of the T_p values considered in this study (i.e. 0.5–10 s). As a consequence, resonance occurs only in torsional response and large values of $\max|ru_\theta(t)|$ are observed. In addition, although the peak value of \tilde{u}_0 for Building A10 is the largest among the three buildings, its peak value of $e_a/2a$ is the smallest. This may be interpreted by the fact that $e_a/2a$ incorporates the combined effects of \tilde{u}_0 and Ω^2 as indicated by Equation (27).
- For Building A36 ($T_x = 1.07$ s), the variation of Ω from 0.5 to 2.0 results in T_θ ranging from 2.14 to 0.54 s, which in turn affects the values of T_p/T_x corresponding to torsional resonance. It should also be noted that, with the exception of $\Omega \approx 1.0$, large values of $|ru_\theta(t')|$ and \tilde{u}_0 are observed when torsional resonance occurs. When $\Omega \approx 1.0$, $|ru_\theta(t')|$ is very small, and \tilde{u}_0 approaches unity, implying that torsional response has a negligible contribution to the increase in building displacements. This trend is schematically explained in Figure 7, where Building A36 with $\Omega = 1.0$ ($T_x = T_\theta = 1.07$ s) is excited by a simplified ground motion pulse. Without loss of generality, let $T_p = 1.2$ s (i.e. to induce torsional resonance), $\gamma = 2.0$ and $\beta = 270$ m/s. Figure 7a compares the phase angles of the transfer functions of translational displacement (U_H/u_{g0}) and displacement due to torsional vibrations ($r\alpha_t/u_{g0}$). Note that the phase of U_H/u_{g0} has been shifted by 90° , yielding a variation of phase angle with normalized frequency that is

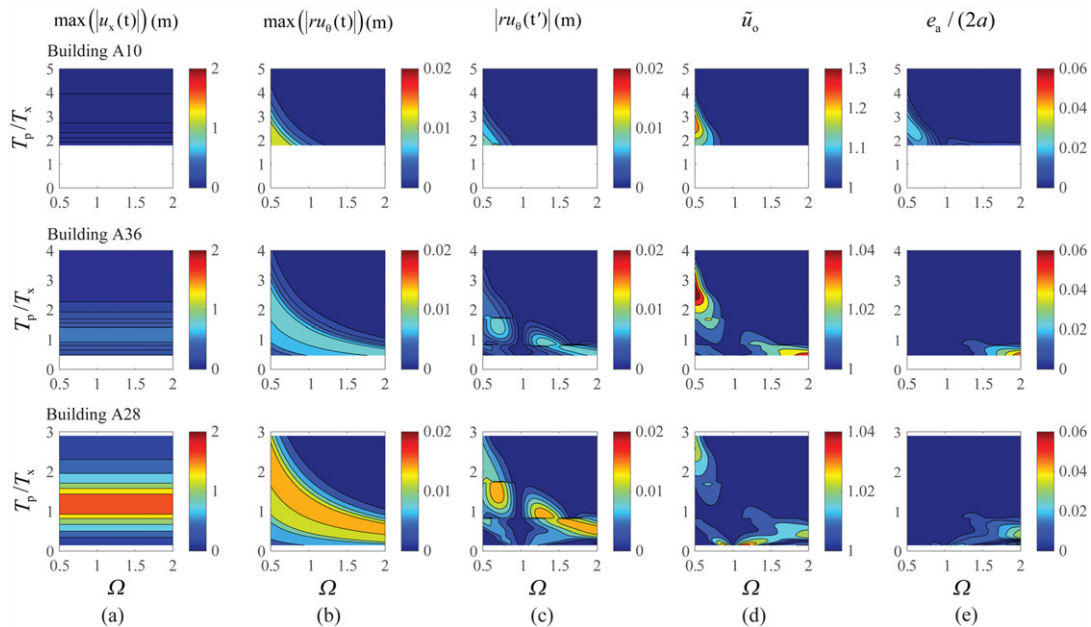


Figure 6. (a) Maximum translational displacement ($\max|u_x(t)|$), (b) maximum displacement due to torsional vibrations ($\max|ru_\theta(t)|$), (c) amplitude of displacement due to torsional vibrations at t' ($|ru_\theta(t')|$), (d) normalized response \tilde{u}_0 , and (e) normalized accidental eccentricity $e_a/2a$ for Buildings A10, A36 and A28 vs. Ω and T_p/T_x . It is assumed that $\beta = 270$ m/s and $\gamma = 2.0$. Note that the lower limit of T_p/T_x differs for each building (see Figure 3), whereas the upper limit of T_p/T_x and the colorbar range are adjusted to emphasize the trends. [Colour figure can be viewed at wileyonlinelibrary.com]

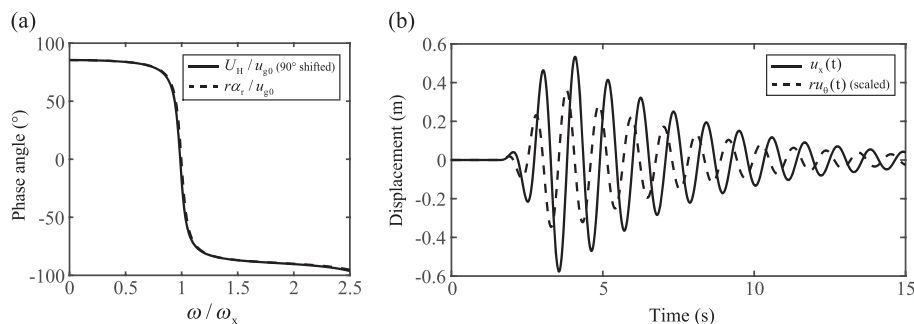


Figure 7. Building A36 with $\Omega = 1.0$ excited by a simplified ground motion pulse with $T_p = 1.2$ s and $\gamma = 2.0$, whereas $\beta = 270$ m/s. (a) Phase angle of transfer functions of translational displacement U_H/u_{g0} (90° shifted) and displacement due to torsional vibrations ra_r/u_{g0} vs. normalized frequency. (b) Time histories of $u_x(t)$ and $ru_{\theta}(t)$, with the latter scaled up by a factor of 40.

almost identical to that of ra_r/u_{g0} . This implies that the torsional response due to wave passage effects is 90° out of phase with respect to the translational response. Figure 7b shows the time histories of $u_x(t)$ and $ru_{\theta}(t)$, with the latter scaled up by a factor of 40 to indicate the waveforms more clearly. It is evident that the two time signals are 90° out of phase, and therefore when u_x attains its peak value, ru_{θ} is close to zero, thus resulting in values of \tilde{u}_0 close to unity. The negligible contribution of the torsional response to the increase in building displacements for buildings with $\Omega \approx 1.0$ has previously been noted by De la Llera and Chopra [7, 33, 34] and is further confirmed in this study.

- For Building A28 ($T_x = 3.45$ s), similar trends can be observed for the variation of $\max|ru_{\theta}(t)|$ and $|ru_{\theta}(t')|$ with respect to Ω and T_p/T_x . However, it is interesting to note that, although local peaks of \tilde{u}_0 are observed when torsional resonance takes place, the global peak of \tilde{u}_0 occurs at $T_p/T_x = 0.14$ (i.e. $T_p = 0.5$ s). This observation can be attributed to higher mode effects. Cao et al. [11] reported local amplification of maximum torsional response for small T_p/T_x values due to the excitation of higher modes, whereas the parametric analysis presented in Section 4 indicated that higher mode effects are relatively insignificant for the maximum translational response. As a consequence, an increased value of \tilde{u}_0 may be obtained, when higher modes are excited.

6.1.2. Effect of parameter γ . Figure 8 shows the normalized accidental eccentricity $e_a/2a$ for Buildings A10, A36, and A28 as a function of Ω and T_p/T_x for $\gamma = 1.0, 1.5, 2.0, 3.0$ and $\beta = 270$ m/s. The variation of γ has a significant effect on the Fourier amplitude spectrum of the ground displacement pulses [12, 11], which in turn affects both the translational and torsional components of the structural response. For Buildings A36 and A28, as γ increases from 1 to 3, the peak values of $e_a/2a$ increase from 0.05 to 0.07 and from 0.03 to 0.08, respectively. However, this trend does not necessarily apply to all buildings (e.g. Building A10 in Figure 8; see also Figure 11). In fact, an increase in γ may result in an increase or decrease in the peak value of $e_a/2a$ depending on the building properties.

6.1.3. Effect of shear wave velocity. For Buildings A10, A36, and A28, the variation of β has negligible effects on $e_a/2a$. This observation can be attributed to the following factors: (i) the torsional response has been found to be controlled by the wave apparent velocity rather than the shear wave velocity [11], and (ii) the maximum translational displacement of these three buildings is generally insensitive to β as shown in Figure 4a. On the other hand, the effects of β on $e_a/2a$ are more noticeable for the three buildings shown in Figure 4b. Figure 9 presents the variation of $e_a/2a$ for Buildings A30, B12, and B3 as a function of Ω and T_p/T_x for $\beta = 170, 270, 560, 1000$ m/s and $\gamma = 2.0$. For a particular building and as β varies, the contours of $e_a/2a$ are of similar shape, indicating that β contributes to the variability of $e_a/2a$ to a lesser extent than other parameters (e.g. Ω , T_p and γ). As β increases, the peak value of $e_a/2a$ increases from 0.15 to 0.21 for Building A30, whereas it decreases from 0.12 to 0.07 for Building B12 and from 0.03 to 0.02 for Building B3.

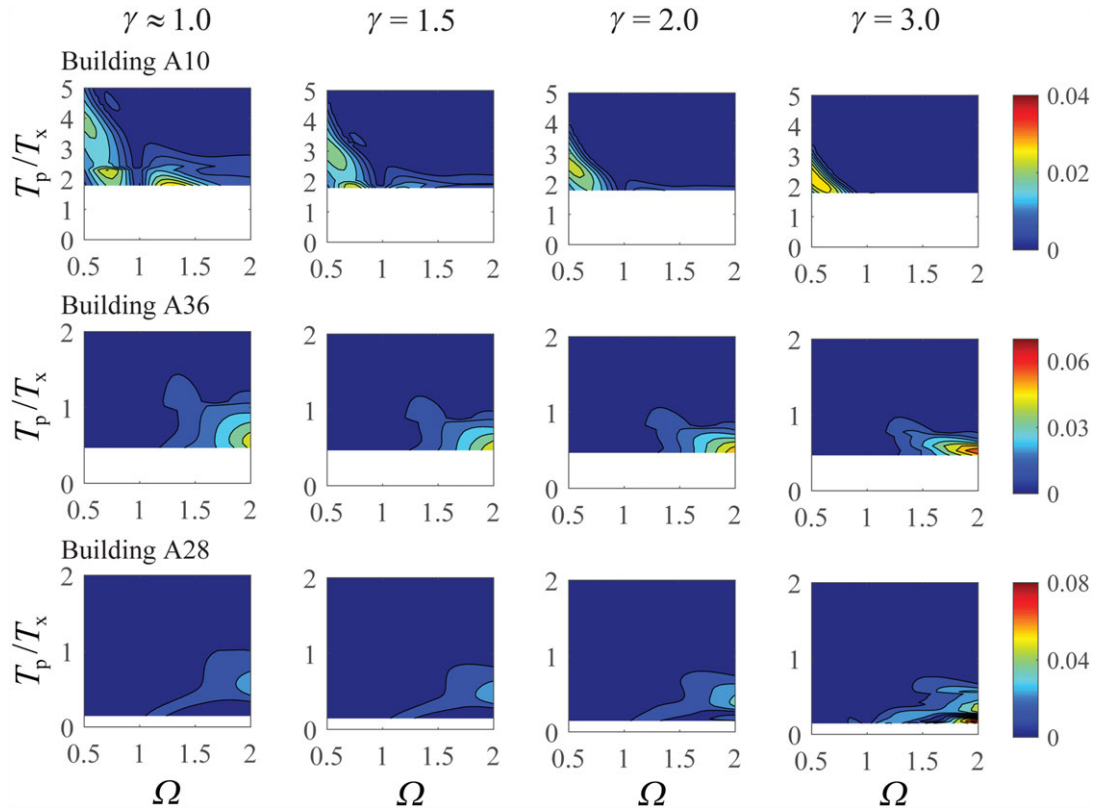


Figure 8. Normalized accidental eccentricity $e_a/2a$ for Buildings A10, A36 and A28 vs. Ω and T_p/T_x for $\gamma = 1.0, 1.5, 2.0, 3.0$ and $\beta = 270$ m/s. Note that the lower limit of T_p/T_x differs for each building (see Figure 3), whereas the upper limit of T_p/T_x and the colorbar range are adjusted to emphasize the trends. [Colour figure can be viewed at wileyonlinelibrary.com]

6.2. Comparison with typical code-prescribed values of accidental eccentricity

Figure 10 shows the variation of $e_a/2a$ for 15 representative buildings as a function of Ω and T_p/T_x for $\beta = 270$ m/s and $\gamma = 2.0$. The contour plots of $e_a/2a$ are displayed in order of increasing T_x (from left to right in rows). Figure 10 indicates that buildings with similar values of T_x exhibit, in general, similar contour plots. In addition, for the majority of buildings, the peak value of $e_a/2a$ tends to occur when T_p/T_x approaches the lower limit of its effective range. On the other hand, the Ω value that corresponds to the peak of $e_a/2a$ varies from 0.5 for buildings with $T_x < 0.4$ s to 2.0 for buildings with $T_x > 0.8$ s. It is worth noting that buildings with larger foundation radius exhibit, in general, larger $e_a/2a$ values. This observation is related to the fact that the displacement due to torsional vibrations is proportional to the foundation radius, and therefore buildings with larger foundation radius are characterized by larger values of \tilde{u}_0 and $e_a/2a$ [7, 10]. Among all 40 buildings, the peak value of $e_a/2a$ exceeds 10% for three buildings and 5% for 11 more buildings.

In generating Figure 10, parameters β and γ were set to fixed values, and therefore the results shown in the figure do not reflect the effect of these two parameters. The shear wave velocity was previously found to have only a limited influence on $e_a/2a$ (see Section 6.1.3). On the other hand, γ affects both the translational and torsional responses and may have an important effect on $e_a/2a$ (see Section 6.1.2). Figure 11a presents the peak values of $e_a/2a$ for all 40 buildings as a function of the foundation radius for $\gamma = 1.0, 1.5, 2.0, 3.0$, $\beta = 270$ m/s, and $\Omega = 0.5-2.0$. Figure 11a suggests that (i) the variation of γ may have a significant effect on $e_a/2a$, but no general trend can be observed, and (ii) there exists a strong tendency of increasing $e_a/2a$ with increasing foundation radius [7, 10]. By taking into consideration the variation of γ , the peak value of $e_a/2a$ exceeds 10% for seven buildings and 5% for 19 more buildings.

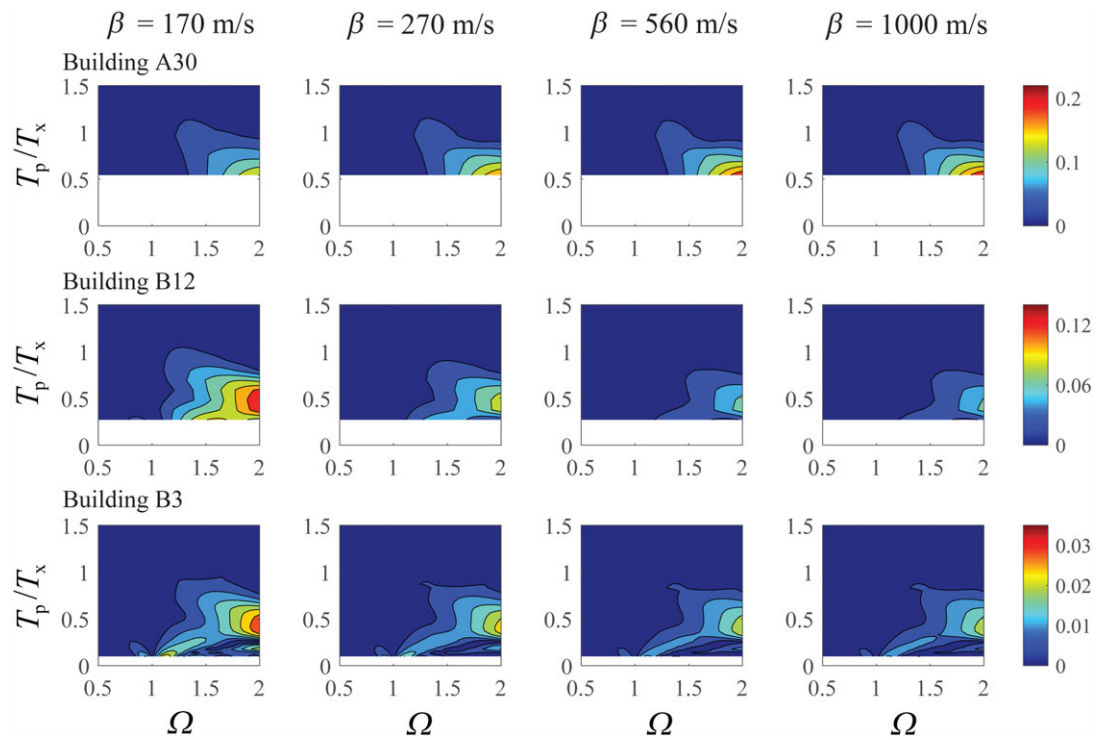


Figure 9. Normalized accidental eccentricity $e_a/2a$ for Buildings A30, B12 and B3 vs. Ω and T_p/T_x for $\beta = 170, 270, 560, 1000$ m/s and $\gamma = 2.0$. Note that the lower limit of T_p/T_x differs for each building (see Figure 4b), whereas the colorbar range is adjusted to emphasize the trends. [Colour figure can be viewed at wileyonlinelibrary.com]

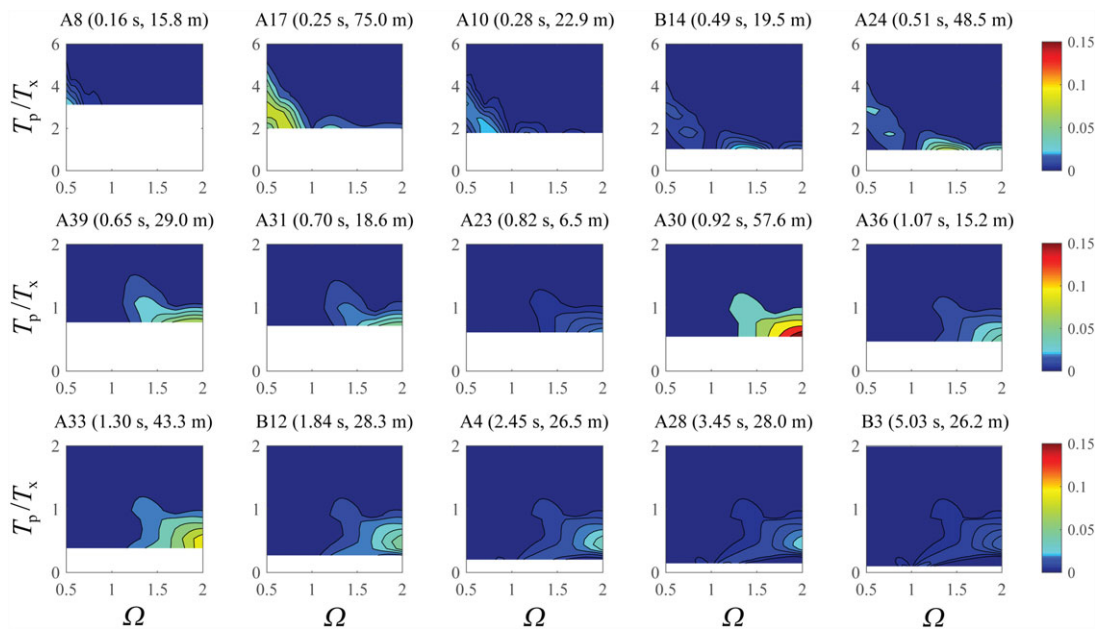


Figure 10. Normalized accidental eccentricity $e_a/2a$ for 15 representative buildings vs. Ω and T_p/T_x for $\beta = 270$ m/s and $\gamma = 2.0$. Buildings are displayed in order of increasing T_x (from left to right in rows). Values within the parentheses denote the fundamental translational period and the foundation radius of each building. Note that the lower limit of T_p/T_x differs for each building, whereas the upper limit of T_p/T_x is adjusted to emphasize the trends. [Colour figure can be viewed at wileyonlinelibrary.com]

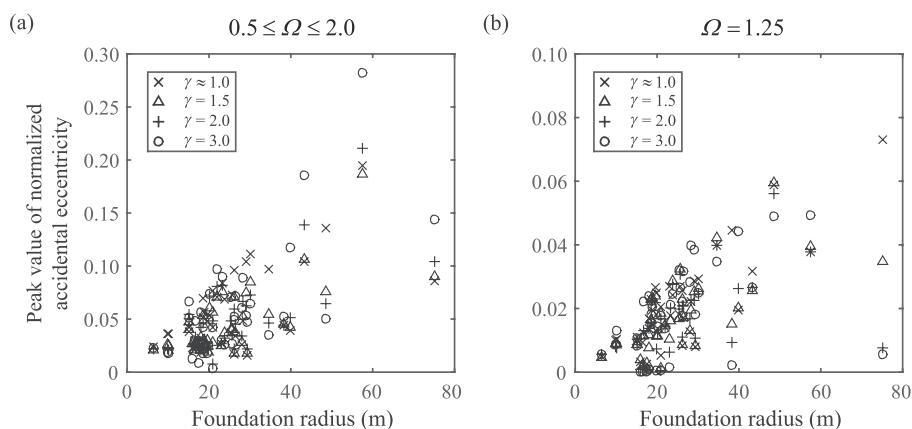


Figure 11. (a) Peak values of normalized accidental eccentricity $e_a/2a$ for all 40 buildings vs. foundation radius for $\gamma = 1.0, 1.5, 2.0, 3.0$, $\beta = 270$ m/s and $\Omega = 0.5\text{--}2.0$. (b) Same as (a), except that $\Omega = 1.25$.

Note that the peak values of $e_a/2a$ shown in Figure 11a were computed for Ω varying between 0.5 and 2.0, thus implying that the majority of buildings attain their peak $e_a/2a$ values at either $\Omega = 0.5$ or 2.0 (according to Figure 10 and the preceding discussion). It may then be argued that the results shown in Figure 11a are not necessarily representative of the most typical design practices of actual buildings because these two extreme values of Ω are relatively uncommon. Following the discussion on the practical range of Ω in Section 5, a value of $\Omega = 1.25$ (i.e. $T_0 = 0.8T_x$) is selected to represent the frequency ratio of realistic buildings. Figure 11b presents the same analysis as in Figure 11a with the exception that Ω is fixed to 1.25. Under this condition, the observations made with regard to Figure 11a still hold true, but the peak values of $e_a/2a$ are significantly smaller. As a matter of fact, it is only for the three buildings (A17, A24, and A30) with the largest foundation radius that the peak value of $e_a/2a$ exceeds 5% for certain values of γ .

6.3. Effect of broadband ground motions

Mavroeidis and Papageorgiou [12] proposed a simplified methodology for generating broadband near-fault pulse-like ground motions adequate for engineering analysis and design. According to this methodology, the coherent (long-period) ground motion component is simulated using the mathematical model presented in Section 2, whereas the incoherent (high-frequency) seismic radiation is synthesized using the specific barrier model [35–37]. Using this approach, Cao et al. [11] simulated time histories of broadband ground motions in the near-fault region for three hypothetical earthquakes of M_W 5.8, 6.4, and 7.0, representing moderate, moderate-to-large, and large seismic events, respectively. These synthetic motions are used in this section to assess the effectiveness of idealized pulse models in estimating the normalized accidental eccentricity.

Figure 12 illustrates the normalized accidental eccentricity $e_a/2a$ for all 40 buildings as a function of T_x for $\Omega = 1.25$ due to the three hypothetical seismic events. For the M_W 5.8, 6.4, and 7.0 earthquakes, the agreement between the values of $e_a/2a$ due to the long-period and broadband ground motions is very good for $T_x > 0.5$ s, 1.0 s and 2.0 s, respectively. For shorter periods, the normalized accidental eccentricity due to the broadband ground motion is clearly underestimated when only the long-period ground motion component is used in the analysis. This observation may be explained by the fact that the seismic response of shorter period buildings is primarily affected by the high-frequency component of the broadband ground motion, implying that the long-period component by itself is not capable of capturing the translational and torsional responses, thus resulting in the observed differences between the computed $e_a/2a$ values.

Figure 12 also shows that short-period buildings ($T_x < 1.0$ s) subjected to broadband ground motions, in general, tend to have larger $e_a/2a$ values than long-period buildings ($T_x > 1.0$ s), especially for the M_W 6.4 and 7.0 earthquakes. In addition, the normalized accidental eccentricities for all 40 buildings subjected to broadband ground motions are less than the typical code-prescribed

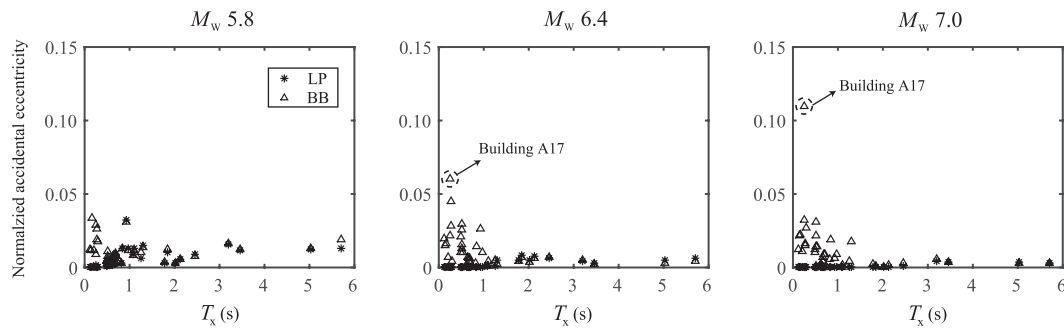


Figure 12. Normalized accidental eccentricity $e_a/2a$ for all 40 buildings as a function of T_x for $\Omega = 1.25$ due to the long-period (LP) and broadband (BB) ground motions of three hypothetical earthquakes.

value of 5%. It is only for Building A17 (circled by dashed line in Figure 12) that $e_a/2a$ reaches values of 6 and 11% for M_w 6.4 and 7.0, respectively. This can be attributed to the 75-m foundation radius of Building A17, which is the largest among all 40 buildings.

7. CONCLUSIONS

This study has investigated the characteristics of the accidental eccentricity in symmetric buildings due to torsional response arising from wave passage effects in the near-fault region. The main contributions and findings of this study are summarized as follows:

- The transfer functions of the translational and rocking response of the foundation and of the translational response of the superstructure were derived analytically assuming that the superstructure behaves as a shear beam under the action of translational and rocking base excitations arising from the propagation of an obliquely incident plane SH wave. Parametric analysis results indicated that the modulus of translational response at the top of the superstructure is primarily sensitive to the slenderness ratio H/a and the relative stiffness parameter a_x for translational vibrations.
- The overall maximum translational displacement due to near-fault pulse-like ground motions is attained when the pulse period T_p of the ground excitation approaches the fundamental translational period T_x of the building and is increased by a factor of ~ 2 as parameter γ increases from 1 to 3. The shear wave velocity β may also have measurable effects on the overall maximum translational displacement depending on parameters a_x and H/a .
- The normalized accidental eccentricity is most sensitive to the pulse period T_p of the near-fault ground motions and to the uncoupled torsional-to-translational fundamental frequency ratio Ω of the structure. Parameter γ may also have a significant effect on the normalized accidental eccentricity, whereas the shear wave velocity β affects the normalized accidental eccentricity to a lesser extent. It was also found that buildings with larger foundation radius exhibit, in general, larger normalized accidental eccentricity.
- The normalized accidental eccentricity due to broadband near-fault ground motions is well approximated by simplified pulse-like ground motions for longer period buildings, while it is underestimated for shorter period buildings. For symmetric buildings with values of Ω commonly used in design practice, the normalized accidental eccentricity due to wave passage effects is less than the typical code-prescribed value of 5%, except for buildings with very large foundation radius.

It should be noted that these findings were obtained for the soil–foundation–structure system considered in this study, i.e., superstructure modeled as a shear beam and foundation represented by a rigid circular disc. Tall slender buildings may experience significant bending, and therefore a model of the superstructure that takes into account both shear and bending deformations should be considered. In addition, further investigation should be carried out considering elongated rectangular

foundations, for which the wave passage effects are expected to be more pronounced. It should also be mentioned that the accidental eccentricity prescribed by building codes is intended to encompass the effects of accidental torsion induced not only from wave passage, but also from ground motion incoherence and uncertainties in the distributions of stiffness and mass. Moreover, nonlinear soil response, ground failure, and soil liquefaction may induce additional transient and permanent rotations on the ground surface near faults [38], which in turn may affect torsional response. Therefore, torsional effects arising from different sources need to be considered to assess the adequacy of code-prescribed values of accidental eccentricity to account for accidental torsion in symmetric buildings subjected to near-fault pulse-like ground motions.

NOMENCLATURE

$A, \gamma, v, f_P,$	Near-fault pulse parameters (amplitude, number of cycles, phase, prevailing frequency,
T_P, t_0	pulse period, time shift)
$V(\omega), D(\omega)$	Fourier transform of ground velocity and displacement signals
H, A, ρ_b	Height, floor area, and mass density of superstructure
a	Foundation radius
m_b, m_0	Masses of superstructure and foundation
I_b, I_0	Mass moments of inertia of superstructure and foundation about z axis
J_0	Mass moment of inertia of foundation about y axis
ω_x, ω_θ	Uncoupled fixed-base fundamental translational and torsional frequencies
ζ_x, ζ_θ	Hysteretic damping factors for translational and torsional vibrations
β, G, σ, ρ_s	Soil properties (shear wave velocity, shear modulus, Poisson's ratio, density)
Θ	Angle of incidence
u_{g0}	Amplitude of free-field motion
U_{gx}^i	Motion of incident wave
U_{gx}^{i+r}	Motion of incident and reflected waves
U_0, Ψ_0	Transfer functions of translational and rocking response of foundation
$U(z)$	Transfer function of translational response of superstructure at level z
U_0^*, Ψ_0^*	Translational and rocking components of foundation input motion
U_s, Ψ_s	Motions of foundation associated with soil deformation
S_{xx}	Frequency-dependent function
a_0	Dimensionless frequency
c_{app}	Wave apparent velocity
V_s, M_s	Force and moment that foundation exerts on soil
$K(\omega)$	Frequency-dependent impedance matrix
$K_{HH}, K_{HM},$ K_{MH}, K_{MM}	Normalized horizontal, coupling, and rocking impedance functions
k	Shear stiffness
m	Mass per unit length
$V(z)$	Shear force at level z
V_b, M_b	Base shear and base moment
a_x, a_θ	Relative stiffness parameters for translational and torsional vibrations
m_s, J_s, I_s	Soil mass and soil moments of inertia
U_H	Transfer function of translational response at top of superstructure
H/a	Slenderness ratio
T_x, T_θ	Fixed-base fundamental translational and torsional periods
δ_m	Foundation-to-superstructure mass ratio
α^*	Foundation input twist
$\alpha_b, \alpha_t, \alpha_r$	Transfer functions of base twist, top twist, and relative twist
θ_R, θ_S	Functions associated with the solution of Fredholm integral equations
Ω	Uncoupled torsional-to-translational fundamental frequency ratio
$u_x(t)$	Translational displacement at top of superstructure

$u_0(t)$	Relative twist between top and base of superstructure
$(\tilde{u}_{\pm r})_0$	Normalized response at $y = \pm r$
\tilde{u}_0	Normalized response defined as $\max\{(\tilde{u}_{\pm r})_0\}$
r	Radius of gyration
$e_a/2a$	Normalized accidental eccentricity
t'	Time instant when \tilde{u}_0 occurs

ACKNOWLEDGMENTS

The first two authors would like to acknowledge financial support provided by the US National Science Foundation under Grant No. CMMI-1360734. The authors also wish to thank two anonymous reviewers for their constructive comments and suggestions that led to improvements in the manuscript.

REFERENCES

1. Anagnostopoulos SA, Kyrkos MT, Stathopoulos KG. Earthquake induced torsion in buildings: Critical review and state of the art. *Earthquakes and Structures* 2015, **8**(2):305–377.
2. Newmark NM. Torsion in symmetrical buildings, in *Proceeding of the Fourth World Conference on Earthquake Engineering*, 1969: Santiago, Chile.
3. Luco JE. Torsional response of structures to obliquely incident seismic SH waves. *Earthquake Engineering and Structural Dynamics* 1976, **4**(3):207–219.
4. Luco JE, Sotiropoulos DA. Local characterization of free-field ground motion and effects of wave passage. *Bulletin of the Seismological Society of America* 1980, **70**(6):2229–2244.
5. Morgan JR, Hall WJ, Newmark NM. Seismic response arising from traveling waves. *Journal of Structural Engineering-ASCE* 1983, **109**(4):1010–1027.
6. Wu ST, Leyendecker EV. Dynamic eccentricity of structures subjected to S–H waves. *Earthquake Engineering and Structural Dynamics* 1984, **12**(5):619–628.
7. De la Llera JC, Chopra AK. Accidental torsion in buildings due to base rotational excitation. *Earthquake Engineering and Structural Dynamics* 1994a, **23**(9):1003–1021.
8. Heredia-Zavoni E, Barranco F. Torsion in symmetric structures due to ground-motion spatial variation. *Journal of Engineering Mechanics-ASCE* 1996, **122**(9):834–843.
9. Heredia-Zavoni E, Leyva A. Torsional response of symmetric buildings to incoherent and phase-delayed earthquake ground motion. *Earthquake Engineering and Structural Dynamics* 2003, **32**(7):1021–1038.
10. Aviles J, Suarez M. Natural and accidental torsion in one-storey structures on elastic foundation under non-vertically incident SH-waves. *Earthquake Engineering and Structural Dynamics* 2006, **35**(7):829–850.
11. Cao Y, Meza-Fajardo KC, Mavroeidis GP, Papageorgiou AS. Effects of wave passage on torsional response of symmetric buildings subjected to near-fault pulse-like ground motions. *Soil Dynamics and Earthquake Engineering* 2016, **88**:109–123.
12. Mavroeidis GP, Papageorgiou AS. A mathematical representation of near-fault ground motions. *Bulletin of the Seismological Society of America* 2003, **93**(3):1099–1131.
13. Halldorsson B, Mavroeidis GP, Papageorgiou AS. Near-fault and far-field strong ground-motion simulation for earthquake engineering applications using the specific barrier model. *Journal of Structural Engineering-ASCE* 2011, **137**(3):433–444.
14. Cork TG, Kim JH, Mavroeidis GP, Kim JK, Halldorsson B, Papageorgiou AS. Effects of tectonic regime and soil conditions on the pulse period of near-fault ground motions. *Soil Dynamics and Earthquake Engineering* 2016, **80**:102–118.
15. Stewart JP, Seed RB, Fenves GL. Seismic soil–structure interaction in buildings. II: Empirical findings. *Journal of Geotechnical and Geoenvironmental Engineering-ASCE* 1999, **125**(1):38–48.
16. Jennings, PC. Earthquake response of tall regular buildings. *Report No. EERL 97-01*, California Institute of Technology, Pasadena, CA, 1997.
17. Meza-Fajardo KC, Papageorgiou AS. Torsional response of structures to impulsive near-fault ground motions, presented at the *99th Annual Meeting of the Seismological Society of America*, 2004: Palm Springs, CA [Abstract in *Seismological Research Letters* 75, pp. 267].
18. Luco JE, Wong HL. Response of structures to nonvertically incident seismic waves. *Bulletin of the Seismological Society of America* 1982, **72**(1):275–302.
19. Luco JE, Mita A. Response of a circular foundation on a uniform half-space to elastic waves. *Earthquake Engineering and Structural Dynamics* 1987, **15**(1):105–118.
20. Iguchi M. An approximate analysis of input motions for rigid embedded foundations. *Transactions of the Architectural Institute of Japan* 1982, **315**:61–75.
21. Wong HL, Luco JE. Dynamic response of rectangular foundations to obliquely incident seismic waves. *Earthquake Engineering and Structural Dynamics* 1978, **6**(1):3–16.

22. Jennings PC, Bielak J. Dynamics of building–soil interaction. *Bulletin of the Seismological Society of America* 1973, **63**(1):9–48.
23. Veletsos AS, Meek JW. Dynamic behavior of building–foundation systems. *Earthquake Engineering and Structural Dynamics* 1974, **3**(2):121–138.
24. Mavroeidis GP, Dong G, Papageorgiou AS. Near-fault ground motions, and the response of elastic and inelastic single-degree-of-freedom (SDOF) systems. *Earthquake Engineering and Structural Dynamics* 2004, **33**(9):1023–1049.
25. Hubbard DT, Mavroeidis GP. Damping coefficients for near-fault ground motion response spectra. *Soil Dynamics and Earthquake Engineering* 2011, **31**(3):401–417.
26. BSSC. NEHRP Recommended Provisions for Seismic Regulations for New Buildings and Other Structures. 2003 edition, Federal Emergency Management Agency, Washington, DC, 2004.
27. Chandler AM, Hutchinson GL. Torsional coupling effects in the earthquake response of asymmetric buildings. *Engineering Structures* 1986, **8**(4):222–236.
28. Riddell R, Santa-Maria H. Inelastic response of one-storey asymmetric-plan systems subjected to bi-directional earthquake motions. *Earthquake Engineering and Structural Dynamics* 1999, **28**(3):273–285.
29. Satake N, Suda K, Arakawa T, Sasaki A, Tamura Y. Damping evaluation using full-scale data of buildings in Japan. *Journal of Structural Engineering-ASCE* 2003, **129**(4):470–477.
30. Lin WH, Chopra AK, De la Llera JC. Accidental torsion in buildings: analysis versus earthquake motions. *Journal of Structural Engineering-ASCE* 2001, **127**(5):475–481.
31. O'Rourke MJ, Bloom MC, Dobry R. Apparent propagation velocity of body waves. *Earthquake Engineering and Structural Dynamics* 1982, **10**(2):283–294.
32. Bouchon M, Aki K. Strain, tilt, and rotation associated with strong ground motion in the vicinity of earthquake faults. *Bulletin of the Seismological Society of America* 1982, **72**(5):1717–1738.
33. De la Llera JC, Chopra AK. Using accidental eccentricity in code-specified static and dynamic analyses of buildings. *Earthquake Engineering and Structural Dynamics* 1994b, **23**(9):947–967.
34. De la Llera JC, Chopra AK. Estimation of accidental torsion effects for seismic design of buildings. *Journal of Structural Engineering-ASCE* 1995, **121**(1):102–114.
35. Papageorgiou AS, Aki K. A specific barrier model for the quantitative description of inhomogeneous faulting and the prediction of strong ground motion. I. Description of the model. *Bulletin of the Seismological Society of America* 1983, **73**(3):693–722.
36. Papageorgiou AS. The barrier model and strong ground motion. *Pure and Applied Geophysics* 2003, **160**:603–634.
37. Halldorsson B, Papageorgiou AS. Calibration of the specific barrier model to earthquakes of different tectonic regions. *Bulletin of the Seismological Society of America* 2005, **95**(4):1276–1300.
38. Trifunac MD. Review: Rotations in structural response. *Bulletin of the Seismological Society of America* 2009, **99**(2B):968–979.